Robotica (1997) volume 15, pp 599–607. Printed in the United Kingdom © 1997 Cambridge University Press

Gait Synthesis for a biped robot

Ching-Long Shih

Department of Electrical Engineering, National Taiwan Institute of Technology, 43, Section 4, Keelung Road, Taipei (Taiwan, 106, R.O.C.)

(Received in final form: January 15, 1997)
E-mail: shih@biped.ee.ntit.edu.tw

SUMMARY

In this paper, the realization of biped walking on even floor, sloping surfaces, and stairs is studied. The motion trajectories for the biped's body and its two feet are modeled by piecewise cubic polynomials. The main features of the biped robot include two variable-length legs and a moving weight which can be positioned side-to-side for balance. The contribution of this paper is gait synthesis and is experimental verification.

KEYWORDS: Biped robot; Gait synthesis; Cubic polynomials; Various surfaces.

1. INTRODUCTION

Multi-legged robots have better terrain adaptability than wheeled mobile robots. Efforts are being made to develop multi-legged locomotion robots for use under extreme difficult environments such as nuclear power plants, in agricultural fields, and on ocean floors. Compared to four-legged or more walking robots, the biped locomotion is expected to be smaller, lighter, and more useful in houses and factories which are designed for smooth human locomotion. Biped robots could be used to help operators in certain tasks that require a certain amount of operator mobility. The function of the body is to carry a load or one or two small manipulators for executing manipulation tasks. In this regard, a useful biped robot should be able to walk on floor, sloping surfaces, and stairs.

Most of the research on bipeds has been actively working to make a robot capable of dynamic walking on even floor. Several prototype biped robots that walk in a dynamically stable manner have been developed. In particular, Miyazaki and Arimoto[1] proposed original reduced-order models that have quantitative relations with the original equations of motion. By setting a simple reference signal function for each controller and using the function repeatedly for each step, stable walking was achieved. Miura and Shimoyama[2] conducted a stability analysis by using an inverted pendulum and developed two biped robots that could walk in a dynamically stable mode. Mita et al.[3] aimed for realizing dynamic biped locomotion by using modern control theory, especially the optimal regulator theory, and conducted plane-walking experiments. In these approaches, the stable walking was achieved by adequate selection of the robot joint trajectories, and having no consideration on the control of the reaction force between the feet and the floor.

Furusho and Sano[4] achieved smooth 3D walking by using a sensor-based control on a biped with nine links. They employed a method to control walking by dividing it into motions in the sagittal plane and the lateral plane. The motion in the lateral plane had a regulator problem with two equilibrium states. For motion in the sagittal plane, they adjusted the body speed close to the smooth speed function given in advance by controlling the ankle torque. The sole and ankle driving actuators underwent a force/torque feedback control based on the sensor information. Li, Takanishi, and Kato[5] used the zero-moment-point (ZMP) as a criterion in order to distinguish the stability of walking for the biped robot WL-12RIII. The assignment of degrees of freedom for their robot is as follows: each of the two hips, the two knees, and the two ankles has one rotational degree of freedom on the pitch axis. The body has three degrees of freedom, in the roll, pitch, and yaw axes. The walking was realized by controlling the body's motion to compensate for the biped walking according to the measured zero-moment-point. Kajita, Yamaura, and Kobayashi[6] used the term "Potential Energy Conserving Orbit" to describe a particular class of trajectories of an ideal biped model. Based on these properties, control laws were formulated for walk initiation, walk continuation, and walk termination. To make their robot legs lighter, four dc motors were mounted in the body, and the legs had parallel link structures. The biped walked an average speed of 20 cm/s.

Generally, the forces exerted on the foot of the supporting leg are the normal reaction forces and friction forces. The reaction forces possess a distributive characteristic and can be always reduced to the resultant. The resultant of the normal distribution forces is the total reaction force and its action point in the walking plane is defined as the ZMP. Shih[7] had built a biped robot capable of statistically and dynamically stable walking on even floor. Because the biped body's speed is not small at the end of a walking cycle, walking on stairs and sloping surfaces was not attempted. That is because the planned trajectory of ZMP is constrained at a fixed point.

Until recently, few studies have investigated biped robots walking on uneven terrain, such as stairs and sloping surfaces. However, the problem is of significant

https://doi.org/10.1017/S0263574797000726 Published online by Cambridge University Press

importance since the motivation to explore the use of legged-robot locomotion is the need for vehicles that can travel on irregular, rough terrain. Zheng and Shen[8] developed a biped robot SD-2 that could climb a sloping surface in a statically stable way. By means of force sensors underneath the foot, their robot was able to detect the transition of the supporting terrain from a flat floor to a sloping surface of up to 10 degrees. Their biped's body leaned forward or backward to compensate for the backward shift of the cg when walking on a slope. McGeer[9] had built a passive biped robot and shown that driven only by gravity, a planar biped robot may be made to walk down a slope. However, without an external source of power, the robot could not stop and stand up. Kajiti and Tani[10] utilized a linearly-inverted pendulum model to control a biped walking on rugged terrain. Because each leg of their biped was configured as a parallel link without an ankle joint, walking on a sloping surface was not attempted. Yamaguchi et al.[11] developed a biped walking robot that adapts to horizontally uneven surfaces by using shock absorbing material to obtain terrain information.

Fewer biped robots can walk on both sloping surfaces and stairs. One of the major problems in designing a biped robot is the difficulty in choosing proper gait for a particular terrain. The proposed approaches here is based on the proper positioning of the biped's body and its two feet by using low level servo control. The trajectories of the body and its feet are modeled by piecewise cubic polynomials. Cubic polynomials are the motion trajectories that minimize the dissipated energy for a double integral dynamic system. The main contribution of this paper is gait synthesis for a biped robot capable of walking on sloping surfaces and stairs, and its experimental verification.

2. MODEL OF THE BIPED ROBOT

In this section, we shall model the biped (named BR-1) based on the single-support case in which one leg is stationary on the floor. The biped robot has two rotational joints on the hip and the ankle joint, as well as one variable-length knee on each leg. One actuator is associated with the body to translate a balance weight in the lateral motion. All of the biped's rotational joints have a gear ratio of 1/160, and the variable-length knee joints have a gear ration of $0.05/\pi$ cm/radian. Because the speed reducers and DC servo motors are considerably heavier than the links of the leg and the frame of the body platform, we assume that the mass of the biped is distributed as four units: the balance weight, the body platform, and two feet. Let

$\boldsymbol{x}_0 = [x_0, y_0, z_0]^T$: location of the body,

$\boldsymbol{x}_1 = [x_1, y_1, z_1]^T$: location of Foot 1,

$\boldsymbol{x}_2 = [x_2, y_2, z_2]^T$: location of Foot 2,

$\boldsymbol{x}_b = [z_0, y_b, z_0]^T$: location of the balance weight,

$\boldsymbol{x}_g = [x_g, y_g, z_g]^T$: center-of-gravity (cg) of the biped,

ϕ_0, ϕ_1, ϕ_2: pitch angle of the body, Foot 1 and Foot 2,

m_b: mass of the balance weight,

m_0: mass of the body including the balance weight,

m_1, m_2: masses of Foot 1 and Foot 2, and

I_0, I_1, I_2: moment of inertia (in Pitch axis) of the biped body, Foot 1 and 2.

Figure 1 shows a schematic representation of the biped kinematic model in the sagittal plane (x–z plane) and in the frontal plane (y–z plane), where α is the inclination angle of the walking surface. The x-axis points to the forward direction, the z-axis points upward, and the y-axis is a cross-product of the z-axis and x-axis. The origin of the base reference coordinate is located at the vertical projection of the center of the body on the ground plane when the biped is in its initial configuration. Let $\boldsymbol{e}_z$ be the unit vector perpendicular to the walking surface, and $\boldsymbol{e}_x$ be the unit vector parallel to the walking direction, and $\boldsymbol{e}_y = \boldsymbol{e}_z \times \boldsymbol{e}_x$. Because the legs are constrained only to swing in the sagittal plane, rotational motion of the biped is allowed only in this plane and $\boldsymbol{e}_y$ is identical with the unit vector of the y-axis. In addition, $y_0 \equiv 0$, $y_1 \equiv w$, and $y_2 \equiv -w$, where w is half of the width of the biped.

The stance of a biped is the configuration itself including the location of its body and the location of each foot with respect to the floor. It is assumed that Leg 1 is the default supporting leg, and hence in this analysis x_1, z_1, and ϕ_1, and ϕ_1 are constants. The dynamic equation of the biped in the work space can be derived from a Langrangian approach[7] as

$$\boldsymbol{M}\ddot{\boldsymbol{p}} + \boldsymbol{G} = \boldsymbol{f}, \tag{1}$$

where

$\boldsymbol{p} = [y_b, x_0, z_0, \phi_0, x_2, z_2, \phi_2]^T$ is the work space position vector,

$\boldsymbol{f} = [f_0, f_1, \ldots, f_6]^T$ is the work space generalized force,

$\boldsymbol{M} = \text{diag}\{m_b, m_0, m_0, I_0, m_2, m_2, I_2\}$, and

$\boldsymbol{G} = [0 \quad 0 \quad m_0 g \quad 0 \quad 0 \quad m_2 g \quad 0]^T$.

To synthesis the biped walking motion, it is required to take a work space variable p from an initial position p_i at time t_i to a final position p_f at time t_f. The motion trajectory for $p(t)$ can be obtained by solving the following optimization problem.

Having the dynamic equation

$$m\ddot{p} + ma = f,$$

determine the motion to minimize the performance index

$$\int_{t_i}^{t_f} \frac{f^2}{2}\, dt$$

subject to the boundary conditions of both $p(t)$ and $\dot{p}(t)$ at time t_i and t_f, where a is either the gravity acceleration or zero.

From the Euler-Language Equation, it can be shown that the resulting solution for $p(t)$ is a cubic polynomial.[12]

https://doi.org/10.1017/S0263574797000726 Published online by Cambridge University Press

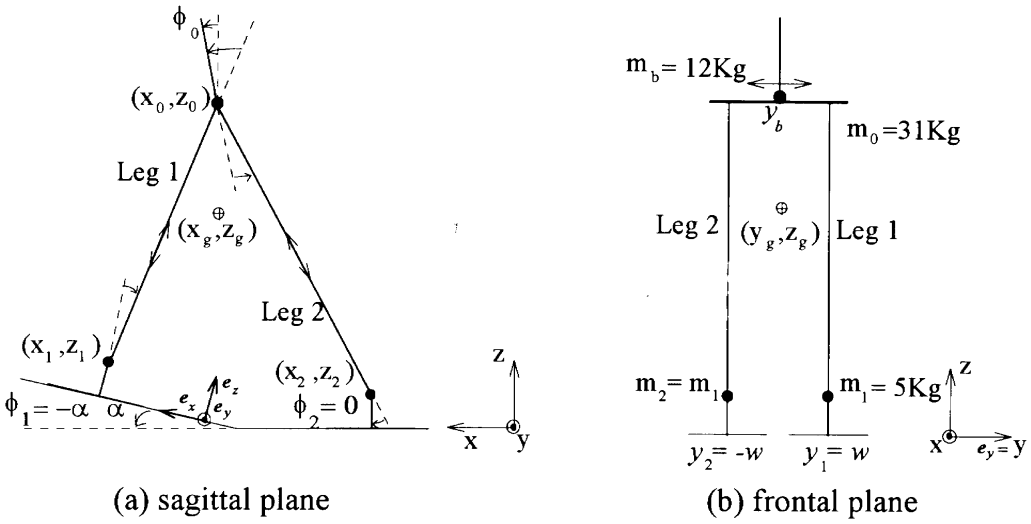


Fig. 1. The kinematic model for the biped BR-1 in (a) the sagittal plane, where α is the incline angle of a sloping surface, and (b) the front plane.

This particular type of trajectory will be used as the basic trajectory for the work space position vector $\boldsymbol{p}$ to plan the biped's walking pattern. Polynomials of third order have the property of being of minimum complexity to allow the positions and velocities at the two ends of a time interval to be freely allocated.

The motions of the biped body and the two feet, in fact, follow an alternating move-and-rest pattern. Thus, a cubic trajectory with zero velocity at both ends of a moving time interval is adequate for the trajectories of the work space variables. The cubic trajectory for a variable $p(t)$ satisfying initial and final values, with rest at both ends of time interval T_p (i.e. $p(0) = p_S$, $p(T_p) = p_T$, and $\dot{p}(0) = \dot{p}(T_p) = 0$), is

$$p(t) = 2(p_S - p_T)\frac{t^3}{T_p^3} + 3(p_T - p_S)\frac{t^2}{T_p^2} + p_S, \quad 0 \le t \le T_p. \tag{2}$$

The acceleration of $p(t)$ is a linear function and its end values are

$$\ddot{p}(T_p) = 6\frac{p_T - p_s}{T_p^2}$$

and

$$\ddot{p}(T_p) = -\ddot{p}(0) = 6\frac{p_s - p_T}{T_p^2}.$$

At the middle of the time interval T_p, we have

$$p(T_p/2) = \frac{p_s + p_T}{2}, \quad \dot{p}(T_p/2) = \frac{3(p_T - p_s)}{2T_p},$$

and

$$\ddot{p}(T_p/2) = 0,$$

where $p(t)$ reaches the half-way point, and has maximum speed and zero acceleration.

3. STATIC BALANCE CONDITIONS

The condition for balance should be considered an important factor in designing a feasible gait pattern, especially for high speed locomotion. Aside from the frictional force, the forces acting on the biped include the gravity force, the inertial force, and reaction force through a planar surface, as well as the inertial moment. Most of the time, the ankle joint motor has to generate a torque to support biped locomotion. This torque must be resisted by the walking surface and the supporting foot.

The total reaction force acting on the biped, $\boldsymbol{N} = [N_x, N_y, N_z]^T$, is

$$\boldsymbol{N} = \begin{bmatrix} m_0\ddot{x}_0 + m_2\ddot{x}_2 \\ m_b\ddot{y}_b \\ m_1 g + m_0(\ddot{z}_0 + g) + m_2(\ddot{z}_2 + g) \end{bmatrix}. \tag{3}$$

The reaction force perpendicular to the surface must be positive during the whole walking cycle so that the foot remains on the slope, i.e., $\boldsymbol{N} \cdot \boldsymbol{e}_z > 0$. The absolute reaction force parallel to the slope must not be large enough for the foot to slide; therefore, it is required that

$$\sqrt{\boldsymbol{N} \cdot \boldsymbol{e}_x^2 + \boldsymbol{N} \cdot \boldsymbol{e}_y^2} \le \mu \boldsymbol{N} \cdot \boldsymbol{e}_z. \tag{4}$$

It is assumed that the frictional coefficient μ is large enough to prevent slippage between the stance foot and the slope during walking.

The resultant total moment, $\boldsymbol{T} = [T_x, T_y, T_z]^T$, of the biped motion measured at the reference point is

$$\boldsymbol{T} = \begin{bmatrix} y_1 m_1 g + y_b m_b(\ddot{z}_0 + g) + y_2 m_2(\ddot{z}_2 + g) - z_0 m_b \ddot{y}_b \\ z_0 m_0 \ddot{x}_0 + z_2 m_2 \ddot{x}_2 - x_0 m_0(\ddot{z}_0 + g) \\ \qquad - x_2 m_2(\ddot{z}_2 + g) + I_0\ddot{\phi}_0 + I_2\ddot{\phi}_2 \\ x_0 m_b \ddot{y}_b - y_b m_b \ddot{x}_0 - y_2 m_2 \ddot{x}_2 \end{bmatrix}. \tag{5}$$

The moments $\boldsymbol{T} \cdot \boldsymbol{e}_x$ and $\boldsymbol{T} \cdot \boldsymbol{e}_y$ must be resisted by the normal surface reaction force $\boldsymbol{N} \cdot \boldsymbol{e}_z$ and the supporting foot to prevent the biped from falling down; therefore, the static balance conditions for the biped in the single-support case are

$$\boldsymbol{N} \cdot \boldsymbol{e}_z(y_1 - d) \le \boldsymbol{T} \cdot \boldsymbol{e}_x \le \boldsymbol{N} \cdot \boldsymbol{e}_z(y_1 + d) \tag{6}$$

and

$$-\boldsymbol{N} \cdot \boldsymbol{e}_z(x_1 + l) \le \boldsymbol{T} \cdot \boldsymbol{e}_y \le -\boldsymbol{N} \cdot \boldsymbol{e}_z(x_1 - l). \tag{7}$$

https://doi.org/10.1017/S0263574797000726 Published online by Cambridge University Press

where l and d are half of the length and the width of the foot, respectively. In other words, the reaction moments $\boldsymbol{T} \cdot \boldsymbol{e}_x$ and $\boldsymbol{T} \cdot \boldsymbol{e}_y$ must not be so large that the foot lifts up from the walking surface. Inequalities (6) and (7) imply that the size of the foot should be large enough to prevent the biped from falling over. However, a large foot may cause interference between the two feet. Furthermore, a large foot will force the biped to walk in a low-speed, statically-stable mode. To reduce the unwanted yawing motion, one may add an additional constant

$$-I_{\max} \le \boldsymbol{T} \cdot \boldsymbol{e}_z \le I_{\max} \tag{8}$$

where $I_{\max}$ is an upper bound for the maximum allowed yawing torque.

4. GAIT SYNTHESIS

In the following analysis, a walking cycle will be regarded as a period of continuous motion while the biped is supported by one foot, followed by an instantaneous impact of the swing foot at the end of the cycle. After impact, the motion is the same as the start of the cycle except that the supporting foot becomes the swing foot and *vice versa.*

4.1. Walking gait for the biped on an even floor

For dynamic walking on an even plane, the walking cycle of the biped can be modeled in three phases, as shown in Figure 2. During Phase 1, the swing leg lifts above the ground. The swing foot moves foward above the ground in Phase 2. Finally, the body moves forward and the swing foot comes back to the ground in Phase 3. During Phase 3, the cg leaves the supporting foot; this shift in the cg actually is characteristic of the biped dynamic walking. Letting T_1, T_2, and T_3 be the time intervals for Phase 1, 2, and 3, respectively, the dynamic walking cycle T then consists of T_1, T_2, and T_3. The above walking pattern can be determined from a set of walking pattern parameters – they are the step size S, the body height H, the swing leg height h, the balance weight traveling distance W, and the time intervals T_1, T_2, and T_3.

It is assumed that the biped's body maintains a constant upright posture during motion, and that both feet stay parallel with the walking floor; therefore,

$$\phi_0 = \phi_1 = \phi_2 = 0.$$

By default, Let 1 is stationary, and hence $x_1 = 0$ and $z_1 = 0$. It is also desired that the body maintains a constant height during walking, i.e. $z_0 = H$. The trajector of Foot 2 can be modeled as below:

$$x_2(t) = \begin{cases} -S & 0 \le t \le T_1 \\ -4S\dfrac{(t-T_1)^3}{(T-\delta T-T_1)^3} & \\ +6S\dfrac{(t-T_1)^2}{(T-\delta T-T_1)^2} - S & T_1 < t \le T-\delta T \end{cases} \tag{9}$$

and

$$z_2(t) = \begin{cases} -2h\dfrac{t^3}{T_1^3} + 3h\dfrac{t^2}{T_1^2} & 0 \le t \le T_1 \\ h & T_1 < t \le T_1 + T_2 \\ 2h\dfrac{(t-T_1-T_2)^3}{T_3^3} & \\ -3h\dfrac{(t-T_1-T_2)^2}{T_3^2} + h & T_1 + T_2 < t \le T \end{cases} . \tag{10}$$

By having a small time interval δT, one can ensure that the swing leg has near zero-forward-velocity when it returns to the floor. Therefore the impact effects can be largely reduced. The biped body and the balance weight

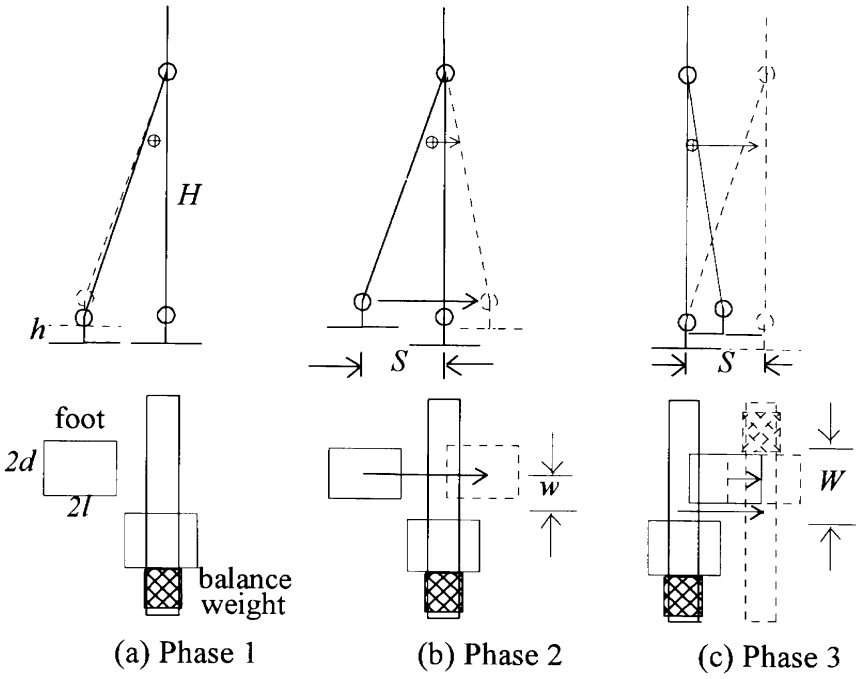


Fig. 2. The dynamic walking cycle of the biped BR-1 in three phases.

https://doi.org/10.1017/S0263574797000726 Published online by Cambridge University Press

start to move at the beginning of Phase 3 and can be modeled by

$$x_0(t) = \begin{cases} 0 & 0 \le t \le T_1 + T_2 \\ -2S\dfrac{(t - T_1 - T_2)^3}{T_3^3} & \\ +3S\dfrac{(t - T_1 - T_2)^2}{T_3^2} & T_1 + T_2 < t \le T \end{cases} \quad (11)$$

and

$$y_b(t) = \begin{cases} W & 0 \le t \le T_1 + T_2 \\ 4W\dfrac{(t - T_1 - T_2)^3}{T_3^3} & \\ -6W\dfrac{(t - T_1 - T_2)^2}{T_3^2} + W & T_1 + T_2 < t \le T \end{cases} \quad (12)$$

To determine a feasible walking pattern, several factors should be considered-they are the position and velocity constraints for work space vector $\boldsymbol{p}$, the static balance conditions for the supporting foot, and the not-falling-down condition for the swing leg.

From the walking gait pattern in Figure 2, the motions of the supporting leg are very limited; therefore, their positions' limits may be neglected. The position constraints for the swing foot can only be checked at both ends of Phase 1. Recalling that the work space trajectory reaches its highest speed at the middle of the move time interval. The velocity constraints can then be checked at the middle of each cubic trajectory time interval.

The static balance constraints of inequalities in (6), (7), and (8) need to be checked at every transition of the three phases. During Phase 3, the projection of the cg moves out of the supporting foot and the body starts to fall, and the swing foot must reach the ground before the biped falls over. Therefore, the high speed of the biped must be maintained during Phase 3. The not-fall-down condition is complicated and not easily obtained. Thus, this constraint is simplified by $T_3 \le T_{\max}$ and is justified by trial-and-error in the walking experiment.

Because the balance weight stays stationary at the top of the stance leg in both Phase 1 and 2, the swing foot can be lifted easily at the beginning of the walking cycle. With the balance weight, we do not need to have the biped's feet cross the center line. Moreover, we do not need to have a supporting mechanism to prevent biped falling over laterally.

4.2. Walking gait for the biped ascending sloping surfaces

For ascending a sloping surface of inclination angle α, the walking cycle of the biped can be modeled in three phases as shown in Figure 3. This walking pattern is reduced to level walking when the inclination angle α is zero. When the robot stands completely on the slope and the body remains vertical to the ground plane, the inclination of the ankle joint represents the gradient of the slope. By default, Leg 1 is the stance leg in the walking cycle; and letting $x_1 = 0$, $z_1 = 0$, $\phi_1 = -\alpha$, and $\phi_0 = 0$. Initially, $x_0 = 0$, $z_0 = H$, $y_b = W$, $x_2 = -S\cos\alpha$, $z_2 = -S\sin\alpha$, and $\phi_2 = -\alpha$, where S is the stride length.

During Phase 1, the swing leg lifts height h above the slope. The swing foot moves forward above and along the slope in Phase 2, and in the mean time the cg remains within the stance foot. Finally, the body moves forward along the slope and the swing foot comes back to the slope in Phase 3. The above walking pattern can be determined from a set of walking pattern parameters –

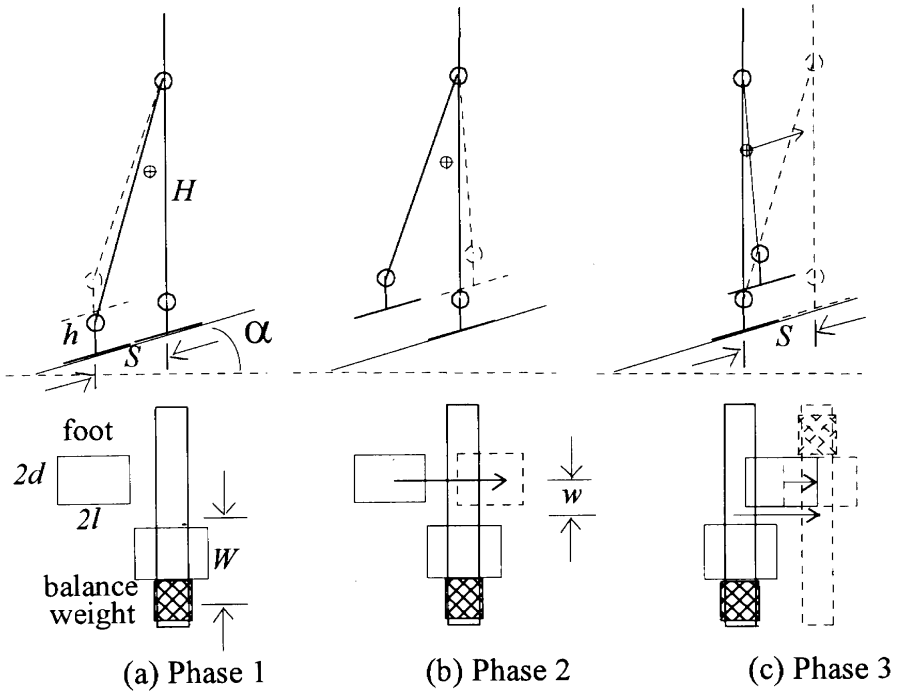


Fig. 3. The walking cycle for biped BR-1 ascending sloping surface in three phases.

https://doi.org/10.1017/S0263574797000726 Published online by Cambridge University Press

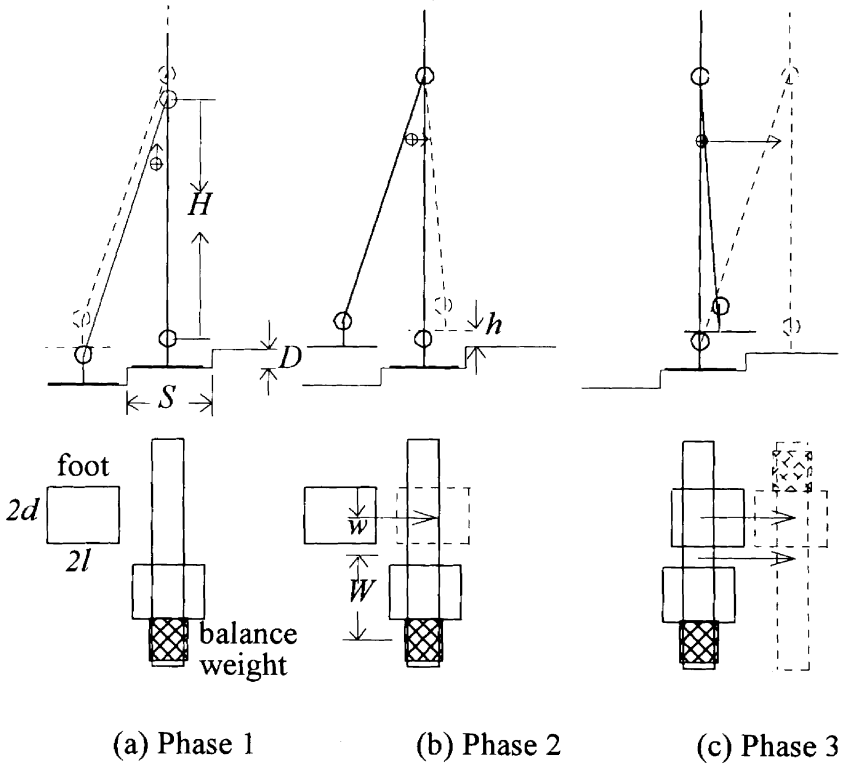


Fig. 4. The walking pattern for biped BR-1 ascending stairs in three phases.

they are the stride length S, the body height H, the swing leg height h, the balance weight traveling distance W, and time intervals T_1, T_2, and T_3. The distance of movement or the step size S depends on the steepness of the slope. In general, the steeper the slope, the smaller the supporting area is, and the more closer the cg is to the boundary of that supporting area.

Foot 2 first lifts itself height h above the slope during Phase 1, then moves forward along the slope in Phase 2, and then finally comes back to the slope surface at Phase 3. The body remains at constant height H during both Phase 1 and Phase 2, and finally moves forward and remains parallel to the slope in Phase 3. The balance weight starts to move from left to right at the beginning of Phase 3. Thus, the positions of position vector $\boldsymbol{p}$ at time instants $t = 0$, T_1, $T_1 + T_2$, and T may be written:

$$\boldsymbol{p}(0) = [-W, 0, H, 0, -S\cos\alpha, -S\sin\alpha, -\alpha]^T,$$

$$\boldsymbol{p}(T_1) = [-W, 0, H, 0, -S\cos\alpha, -S\sin\alpha + h, -\alpha]^T,$$

$$\boldsymbol{p}(T_1 + T_2) = [-W, 0, H, 0, x_2(T_1 + T_2), h, -\alpha]^T,$$

and

$$\boldsymbol{p}(T) = [W, S\cos\alpha, H + S\sin\alpha, 0, S\cos\alpha, S\sin\alpha, -\alpha]^T.$$

Note that $x_2(T_1 + T_2)$ depends on the duration of intervals T_2, δT, and T_3. By specifying that the velocities of $\boldsymbol{p}$ be zero at the above corresponding time instants (i.e. $\dot{\boldsymbol{p}}(0) = 0$, $\dot{\boldsymbol{p}}(T_1) = 0$, $\dot{\boldsymbol{p}}(T_1 + T_2) = [0, 0, 0, 0, \dot{x}_2(T_1 + T_2), 0, 0]^T$, and $\dot{\boldsymbol{p}}(T) = 0$), the trajectories for Foot 2, the body, and the balance weight can then be modeled by piece-wise cubic polynomials. A similar procedure for determining level walking parameters can be applied to determine a feasible walking pattern for the biped ascending a sloping surface. Biped BR-1's walking pattern for descending a sloping surface with inclination angle α can be planned in a similar way. The descending motion derivation is based on the biped moving backward on an up-right sloping surface.

4.3. Walking gait for the biped ascending stairs

For ascending stairs in which the stair size S and the stair height is D, the walking cycle of the biped can also be modeled in three phases as shown in Figure 4. The proposed biped walking pattern for ascending stairs has both an ease and simplicity of implementation. By default, Leg 1 is stationary during the walking time interval T, and $x_1 = 0$, $z_1 = 0$, and $\phi_0 = \phi_1 = \phi_2 = 0$. Initially, $x_0 = 0$, $z_0 = H$, $x_2 = -S$, $z_2 = -D$, $y_b = W$.

During Phase 1, the body moves height D up the stairs simultaneously and the swing leg lifts above the stairs. The motivation of Phase 1 is for the biped to adapt the stairs by simply utilizing its variable-length knees. After Phase 1, the rest of the cycle can be treated as level walking. The swing foot moves forward above the stairs in Phase 2, and in the mean time the cg remains within the stance foot. finally, the body moves forward and the swing foot comes back to the stairs in Phase 3. The above walking pattern can be determined from a set of walking pattern parameters – they are the body height H, the swing leg height h, the balance weight traveling distance W, and the time intervals T_1, T_2, and T_3. Due to the foot size, the stair side S must be longer than the foot length $2l$, and the height D of the stairs is limited by the traveling range of the knee joint.

Foot 2 first lifts itself height h above the stairs during Phase 1, then moves forward and up to height $D + h$ in Phase 2, and then finally comes back to the stairs at

https://doi.org/10.1017/S0263574797000726 Published online by Cambridge University Press

Phase 3. The body first moves height D up the stairs during Phase 1, and then remains at constant height $H + D$ during Phase 2, and finally moves forward horizontally in Phase 3. The balance weight starts to move from left to right at the beginning of Phase 3. Thus, the positions of position vector $\boldsymbol{p}$ at time instants $t = 0$, T_1, $T_1 + T_2$, and T may be written:

$$\boldsymbol{p}(0) = [-W, 0, H, 0, -S, -D, 0]^T,$$
$$\boldsymbol{p}(T_1) = [-W, 0, H + D, 0, -S, h, 0]^T,$$
$$\boldsymbol{p}(T_1 + T_2) = [-W, 0, H + D, 0, x_2(T_1 + T_2), h + D, 0]^T,$$

and

$$\boldsymbol{p}(T) = [W, S, H + D, 0, S, D, 0]^T.$$

By specifying that the velocities of $\boldsymbol{p}$ be zero at the above corresponding time instants, the trajectories for Foot 2, the body, and the balance weight can be modeled by piece-wise cubic polynomials. The walking pattern of descending stairs for biped BR1 can also be planned in a similar way.

5. EXPERIMENTRAL WALKING

The biped's motion control is designed to track a commanded path which is calculated in advance. The biped's motion control is realized by a hierarchical control structure, in which trajectory planning for the walking pattern is executed at the upper level and the servo control for the planned trajectory is executed at the lower level. The servo control part is set up to follow the planned trajectory so that a stable walking motion is realized. The commanded joint trajectory for biped BR-1 is obtained by using a cubic B-spline data interpolation technique. First, each work space command point is converted to a knot point in the joint space by the inverse kinematics. Then, cubic B-spline trajectories which blend together the series of knots serve as the commanded joint position trajectories.

Figure 5 shows the experimental biped walking robot BR-1, consisting of a body and two variable-length legs, which has been designed and built at the National Taiwan Institute of Technology. Walking on an even floor, ascending and descending stairs, and walking from an even floor to a sloping surface and vice versa were all recorded successfully on the video tape.[13,14] The limits on the travel distance were constrained by the length of the tether line connected to the off-board computer and drivers rather than the methodology itself.

In the level walking experiments, the biped BR-1 moved forward and backward which included walk initiation, two continuous walking cycles, and walk termination. The walking pattern parameters are selected as follows: $S = 0.20$ m, $h = 0.03$ m, $W = 0.135$ m, $T_1 = 0.4$ seconds, $\delta T = 0.05$ seconds, and $T_2 = T_3 = 0.8$ seconds. Figure 6 shows a sequence of experimental stick diagrams when the biped walking on evern floor. The motion speed is mostly limited by the velocity of the knee joint, which has the largest gear reduction among the joints of the biped.

In the ascending and descending sloping surfaces experiment, the biped initially stood on level ground with the incline equal to zero. Biped BR-1 then moved up three strides from the level ground to up the slope, and moved three strides down the sloping surface from the slope to the level ground. Because the supporting area becomes smaller, the biped may easily to slip when ascending the slope. To prevent the biped's slippage, the walking surface is covered by a rubber pad. By considering all constraints, one can choose walking parameters as follows: $S = 0.20$ m, $H = 0.520$ m, $h = 0.03$ m, $W = 0.135$ m, $T_1 = 0.5$ seconds, $T_2 = 1.0$ seconds, $\delta T = 0.05$ seconds and $T_3 = 1.0$ seconds for biped BR-1 to ascend the sloping surface with inclination angle $\alpha = 10$ degrees. Figure 7 shows the sequence of experimental stick diagrams when the biped ascending the sliping surface. Figure 8 shows a sequence of experimental stick diagrams when the biped descending the sloping surface. The same walking parameters for the ascending motion are chosen for the descending motion except $H = 0.540$ m. The robot demonstrated stable walking for both ascending and descending of slopes. For both walking up and down the slope, the robot had a speed of one step per 2.5 seconds with step size of being 20 cm. During the ascending/descending slope walking,

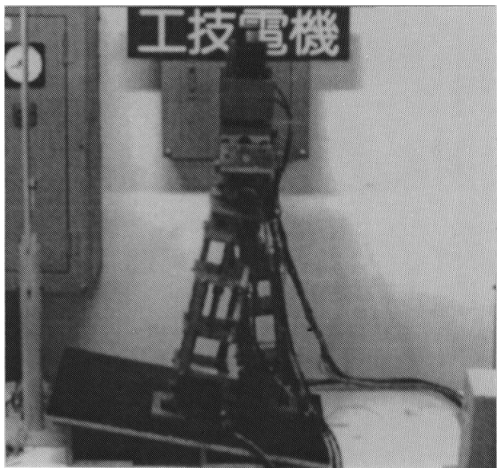


Fig. 5. The prototype biped BR-1 ascending a sloping surface during the experiment.

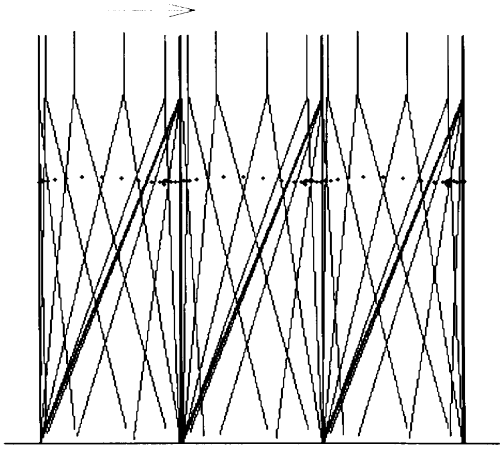


Fig. 6. Biped stick diagrams in the level walking experiment. The small circles denote the cg's trajectory.

https://doi.org/10.1017/S0263574797000726 Published online by Cambridge University Press

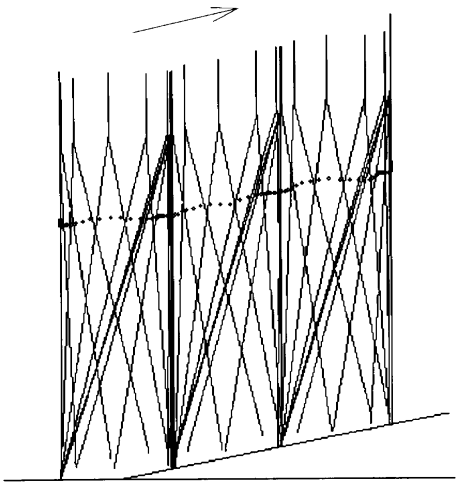


Fig. 7. The biped's stick diagrams in the ascending a sloping surface experiment. The small circles denote the cg's trajectory.

the total variations in the joint variables during the motion for walking down the slope are much smaller than for walking up the slope. Therefore, the motion for descending a slope consumes less energy and may be walk faster than the ascending motion. In an extreme case, a planar biped did walk down a shallow slope without an external source of power.[9]

In the ascending and descending stairs experiment, biped BR-1 moved up and moved down three stairs. The stairs are characterized by length $S = 24$ cm and height $D = 4$ cm. The walking pattern parameters are chosen as follows: $H = 0.515$ m, $h = 0.03$ m, $W = 0.135$ m, $T_1 =$ 1.0 second, $\delta T = 0.05$ seconds, $T_2 = 1.0$ seconds, and $T_3 = 1.0$ seconds. Figure 9 shows the sequence of experimental stick diagrams when the biped ascending stairs. The walking pattern parameters for descending stairs are chosen as follows: $H = 0.515$ m, $h = 0.03$ m, $W = 0.135$ m, $T_1 = 1.0$ second, $T_2 = 1.45$ seconds, and $T_3 = 1.50$ seconds. Figure 10 shows a sequence of experimental stick diagrams when the biped descending stairs. Slower motion and a heavier impact occur when descending stairs.

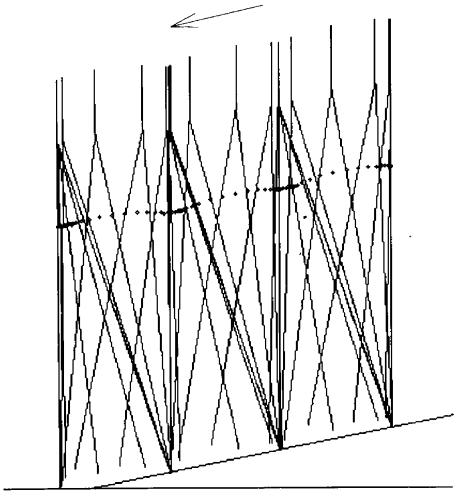


Fig. 8. The biped's stick diagrams in the descending a sloping surface experiment. The small circles denote the cg's trajectory.

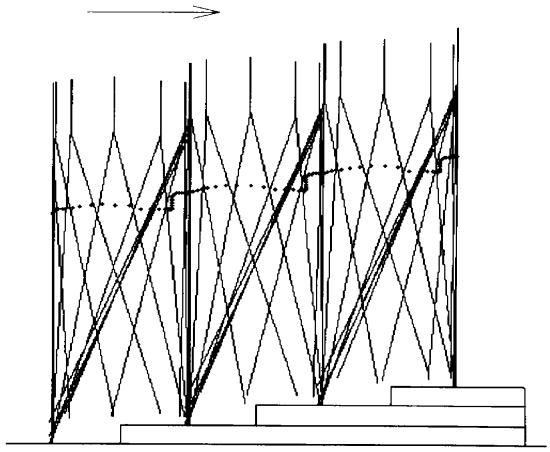


Fig. 9. Biped's stick diagrams in the ascending stairs experiment. The small circles denote the cg's trajectory.

Except for the variations of knee joints and the height of the swing feet, the above biped walking experiments are matched with theoretical results. The slowness of the knee joints result because they have the largest gear ratio among the joints. This downshift of the swing foot is mainly due to the gravity of the biped body, which contributes most of the weight of the biped.

During the walking experiment, the final speed and acceleration of the swing foot may not be zero; therefore, an impact with the floor occurs. To overcome this problem, the walking cycle should not exceed a limit (e.g. 2.0 seconds in our experiment), and it is required that the biped paused for a finite time interval before starting the next walking cycle. It was shown that the biped had to slow down its motion at the end of a walking cycle and to reach statically stable posture. To slow down the biped, a short pause between two continuous cycles is effective like we did in the experiment. This short pause adds an additional impact phase in the walking cycle. Thus, when the biped walks it still suffers from an unsmooth motion of the cg in the walking experiment.

The proposed biped gait patterns are not optimal in the sense of speed and the smoothness of the trajectory;

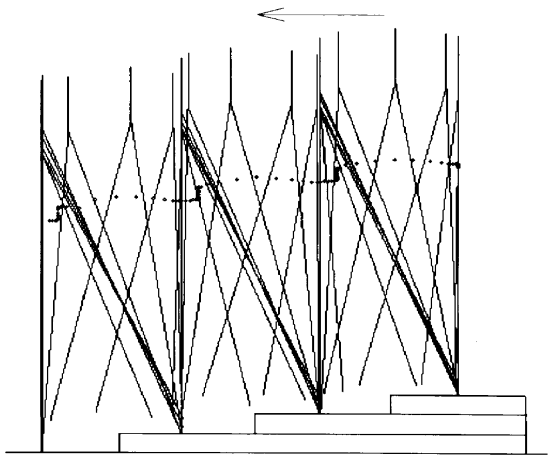


Fig. 10. Biped's stick diagrams in the descending stairs experiment. The small circles denote the cg's trajectory.

https://doi.org/10.1017/S0263574797000726 Published online by Cambridge University Press

however, it is easy to implement. The proposed walking gaits can be transferred to the statically stable mode by placing the swing foot on the floor before the biped's body moves forward in Phase 3. Although the speed is slower when biped BR-1 walks in a statically stable manner, a safer and less energy-consuming motion can be expected.

6. CONCLUSIONS

The effectiveness of the gait synthesis for the biped walking on an even floor, a sloping surface, and on stairs has been experimentally supported. Experiments with biped BR-1 show that overall walking scheme is simple to implement and it requires only low level servo control. Our current hardware system provides only the joint's position and velocity feedback; therefore, the biped's walk is an open-loop.

ACKNOWLEDGEMENT

This work was supported by the National Science Council of Taiwan under Grant NSC85-2213-E-011-049.

References

1. F. Miyazaki and S. Arimoto, "A Control Theoretic Study on Dynamical Biped Locomotion," *ASME Journal of Dynamics, Systems, Measurement and Control,* **102,** 233–239 (1980).
2. H. Miura and I. Shimoyama, "Dynamic Walk of Biped Locomotion," *Int. J. Robotics Research* **3,** No. 2, 60–74, (1984).
3. T. Mita, T. Yamaguchi, T. Kashiwase and T. Kawase, "Realization of a High Speed Biped Using Modern Control Theory," *Int. J. of Control* **40,** No. 1, 107–119 (1984).
4. J. Furusho and A. Sano, "Sensor-Based Control of a Nine-Link Biped," *Int. J. Robotics Research* **9,** No. 2, 83–98 (1990).
5. Q. Li, A. Takanishi and I. Kato, "A Biped Walking Robot Having a ZMP Measurements System Using Universal Force-Moment Sensors," *IEEE/RSJ Intel. Workshop on Intelligent Robots and Systems IROS'91,* Osaka, Japan (1991) pp. 1568–1573.
6. S. Kajita, T. Yamaura and A. Kobayashi, "Dynamic Walking Control of a Biped Robot along a Potential Energy Conserving Orbit," *IEEE Trans. on Robotics and Automation* **8,** No. 4, 431–438 (1992).
7. C.L. Shih, "The Dynamics and Control of a Biped Walking Robot With Seven Degrees of Freedom," *ASME Journal of Dynamic Systems, Measurement, and Control* **118,** No. 4 683–690 (1996).
8. Y. Zheng and J. Shen, "Gait Synthesis for the SD-2 Biped Robot to Climb Sloped Surface," *IEEE Trans. on Robotics and Automation* **6,** No. 1, 86–96 (1990).
9. T. McGeer, "Passive Dynamic Walking," *Int. J. Robotics Research* **9,** No. 2, 62–82 (1990).
10. S. Kajita and K. Tani, "Study of Dynamic Biped Locomotion on Rugged Terrain-Derivation and Application of the Linear Inverted Pendulum Mode," *Proc. IEEE Inter. Conf. Robotics and Automation,* (1991) pp. 1405–1411.
11. J. Yamaguchi, A. Takanishi and I. Kato, "Development of a Biped Walking Robot Adapting to a Horizontally Uneven Surface," *IROS* (1994) pp. 1156–1163.
12. D.E. Kirk, *Optimal Control Theory – An Introduction* (Prentice-Hall, USA, 1970).
13. C.L. Shih and C.J. Chiou, "Statically Stable Walking of a Biped Robot with Seven Degrees of Freedoms," *Video Proceeding 1996 IEEE International Conference on Robotics and Automationn,* Minneapolis, Minnesota, USA (1996) pp. 19–20.
14. C.L. Shih, "Experimental Walking of a Biped Robot," *Video Proceeding 1996 IEEE International Conference on Industrial Electronics, Control, and Instrumentation, IECON'96,* Taipei, Taiwan (1996) p. 8.

https://doi.org/10.1017/S0263574797000726 Published online by Cambridge University Press